Functional Analysis of the Arabidopsis *TETRASPANIN* Gene Family in Plant Growth and Development[1][OPEN]

Feng Wang, Antonella Muto, Jan Van de Velde, Pia Neyt, Kristiina Himanen[2], Klaas Vandepoele, and Mieke Van Lijsebettens*

Department of Plant Systems Biology, VIB, B–9052 Ghent, Belgium (F.W, A.M., J.V.d.V., P.N., K.H., K.V., M.V.L.); Department of Plant Biotechnology and Bioinformatics, Ghent University, B–9052 Ghent, Belgium (F.W, A.M., J.V.d.V., P.N., K.H., K.V., M.V.L.); and Department of Biology, Ecology and Earth Sciences, University of Calabria, 87036 Arcavacata of Rende, Italy (A.M.)

ORCID IDs: 0000-0003-4975-9467 (K.H.); 0000-0003-4790-2725 (K.V.); 0000-0002-7632-1463 (M.V.L.).

TETRASPANIN (*TET*) genes encode conserved integral membrane proteins that are known in animals to function in cellular communication during gamete fusion, immunity reaction, and pathogen recognition. In plants, functional information is limited to one of the 17 members of the Arabidopsis (*Arabidopsis thaliana*) *TET* gene family and to expression data in reproductive stages. Here, the promoter activity of all 17 Arabidopsis *TET* genes was investigated by *pAtTET*::*NUCLEAR LOCALIZATION SIGNAL-GREEN FLUORESCENT PROTEIN/β-GLUCURONIDASE* reporter lines throughout the life cycle, which predicted functional divergence in the paralogous genes per clade. However, partial overlap was observed for many *TET* genes across the clades, correlating with few phenotypes in single mutants and, therefore, requiring double mutant combinations for functional investigation. Mutational analysis showed a role for *TET13* in primary root growth and lateral root development and redundant roles for *TET5* and *TET6* in leaf and root growth through negative regulation of cell proliferation. Strikingly, a number of *TET* genes were expressed in embryonic and seedling progenitor cells and remained expressed until the differentiation state in the mature plant, suggesting a dynamic function over developmental stages. The cis-regulatory elements together with transcription factor-binding data provided molecular insight into the sites, conditions, and perturbations that affect *TET* gene expression and positioned the *TET* genes in different molecular pathways; the data represent a hypothesis-generating resource for further functional analyses.

During embryogenesis in plants, the fertilized egg cell develops gradually by consecutive, but partially overlapping, processes, such as cell division, patterning, and growth, into the rudimentary body plan of the mature embryo. Early pattern formation in the embryo generates the body plan polarity, with apical and basal stem cell progenitor domains, and the different concentric progenitor tissue layers, in which cells interpret their position, acquire cell fate, and differentiate into specific morphologies and functions after germination. Then, the apical meristems are activated to generate the primary root and the aboveground vegetative structures (Murray et al., 2012; Perilli et al., 2012). In the seedling, patterning processes occur in the epidermis to generate specialized cells such as trichomes and stomata, in the shoot apical meristem (SAM) upon leaf initiation and in the primary root pericycle upon lateral root initiation. Developmental programs such as germination, photomorphogenesis, and floral transition occur in response to environmental stimuli, such as light, circadian clock, and temperature, and hormonal stimuli that require cellular communication and signaling. Membrane proteins, located at the plasma membrane, are the most upstream components in signaling perception and transduction during cellular communication. It is estimated that 20% to 30% of all genes in most genomes encode integral proteins (Krogh et al., 2001), which are transmembrane proteins.

Tetraspanins are a distinct class of conserved integral proteins with four transmembrane domains, a small extracellular loop, and a large, Cys-rich extracellular loop, which is important for interacting with each other and other proteins to form tetraspanin-enriched microdomains that participate in cell-to-cell communication

[1] This work was supported by the China Scholarship Council (predoctoral fellowship to F.W.), the Ministero dell'Istruzione, dell'Università e della Ricerca (MIUR; predoctoral fellowship to A.M.), the Multidisciplinary Research Partnership "Bioinformatics: From Nucleotides to Networks" of Ghent University (grant no. 01MR0410W to K.V.), and the Agency for Innovation by Science and Technology in Flanders (predoctoral fellowship to J.V.d.V.).

[2] Present address: Department of Agricultural Sciences, University of Helsinki, Latokartanonkaari 7, 00790 Helsinki, Finland.

* Address correspondence to mieke.vanlijsebettens@psb.vib-ugent.be.

The author responsible for distribution of materials integral to the findings presented in this article in accordance with the policy described in the Instructions for Authors (www.plantphysiol.org) is: Mieke Van Lijsebettens (mieke.vanlijsebettens@psb.vib-ugent.be).

F.W. designed, performed, and interpreted the experiments and wrote the article; A.M. and P.N. performed the experiments; J.V.d.V. and K.V. designed, performed, and interpreted the bioinformatic analyses and wrote the article; K.H. designed and interpreted the experiments; M.V.L. designed the project and experimental approach, coordinated the work, and wrote the article.

[OPEN] Articles can be viewed without a subscription.

www.plantphysiol.org/cgi/doi/10.1104/pp.15.01310

processes during cell morphogenesis, motility, and fusion (Yáñez-Mó et al., 2009). Tetraspanins comprise large gene families in multicellular organisms: 33 in human and 36 in *Drosophila melanogaster* (Huang et al., 2005). Mutations in animal tetraspanins result in severe defects, such as incurable blindness and impaired fertility (Kaji et al., 2002; Goldberg, 2006). In plants, phylogenetic studies identified 17 tetraspanin genes in the Arabidopsis (*Arabidopsis thaliana*) genome, most of which are duplicated (Cnops et al., 2006; Wang et al., 2012; Boavida et al., 2013). Mutants of the Arabidopsis *TETRASPANIN1/TORNADO2/EKEKO* (*TET1/TRN2*) show defects in leaf lamina symmetry and venation pattern, root epidermal patterning (Cnops et al., 2000, 2006), peripheral zone identity of the SAM (Chiu et al., 2007), and megasporogenesis (Lieber et al., 2011). A number of Arabidopsis tetraspanins are expressed in reproductive tissues and at fertilization, and are localized at the plasma membrane of protoplasts (Boavida et al., 2013). However, a systematic analysis of all members of the plant *TET* gene family in embryonic and vegetative development and upon hormonal and environmental stimuli is lacking.

Here, the 17 members of the Arabidopsis *TET* gene family were analyzed for their cellular expression during embryonic and vegetative development by *pAtTET1-17*::*NUCLEAR LOCALIZATION SIGNAL* (*NLS*)*-GFP/GUS* reporter lines, which was instrumental for further mutational analyses. Indeed, a role for *TET13* in primary root growth and lateral root development and redundant roles for *TET5* and *TET6* in leaf and root growth were identified, as suggested by the site of their expression. Complementary experimental and computational regulatory data sets were integrated to identify putative cis-regulatory elements in the *TET* promoters. A transcription factor (TF)-*TET* gene regulatory network was delineated, and regulatory interactions were confirmed by perturbation expression data.

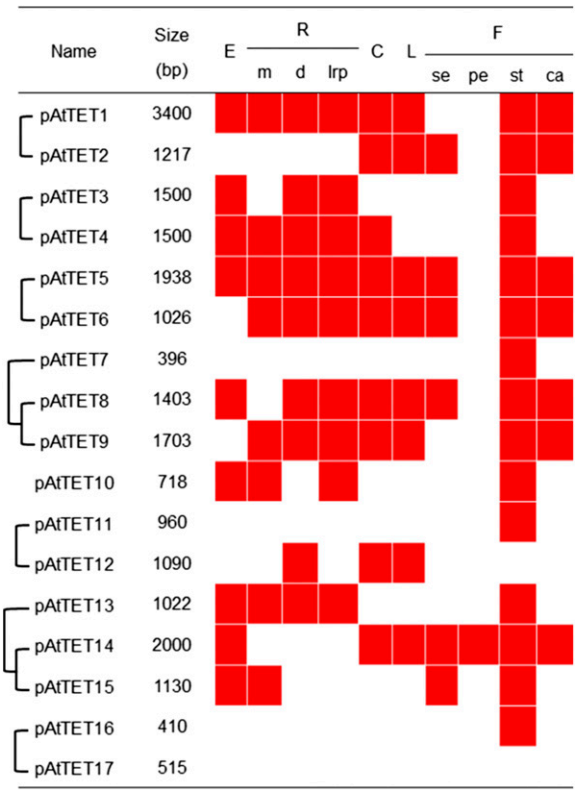

Figure 1. Schematic overview of *TET* expression patterns in different organs. Duplicated gene pairs are indicated with square brackets. (The length of the square brackets does not represent the evolutionary distance.) E, Embryo; R, root; m, primary root meristem and root tip; d, primary root differentiation zone; lrp, lateral root primordia; C, cotyledon; L, rosette leaf; F, flower; se, sepal; pe, petal; st, stamen; ca, carpel.

RESULTS

Expression of *TET* Genes in Specific Tissues, Domains, and Cells throughout the Plant's Life Cycle

The promoter activities of the 17 *TET* gene family members were analyzed by *pAtTET*::*NLS-GFP/GUS* lines throughout the life cycle in order to reveal their site and timing of activity and help in designing further mutational analyses. Per *TET* gene, at least three independent T2 *pAtTET*::*NLS-GFP/GUS* lines, with a single-locus insertion, were analyzed by 5-bromo-4-chloro-3-indolyl-β-D-glucuronide (X-Gluc) histochemical staining in embryo, root, leaf, and flower organs. None of the *TET* genes was expressed in all organs, and only a few had similar expression patterns (Fig. 1). Moreover, within a specific organ, *TET* gene expression was not constitutive but restricted to specific domains, tissues, or cell types.

Nine *TET* genes (i.e. *TET1*, *TET3*, *TET4*, *TET5*, *TET8*, *TET10*, *TET13*, *TET14*, and *TET15*) were expressed in the early globular and heart stage embryo, in which patterning takes place (Fig. 2). *TET3* was expressed in the SAM progenitor domain of all embryo stages, *TET13* in the hypophysis, and *TET15* in the basal part of the embryo, including the hypophysis, suggesting that *TET3*, *TET13*, and *TET15* might participate in apical-basal patterning. *TET1* was asymmetrically expressed in vascular tissue precursor cells of the heart stage embryo. *TET5* expression was restricted to vascular tissue progenitor cells in the center of the globular, heart, and torpedo stage embryo, a pattern similar to that of *TARGET OF MONOPTEROS5*, which is necessary for periclinal cell division and vascular tissue initiation (De Rybel et al., 2013). *TET4* and *TET10* were expressed in the central part of the embryo, including the vascular bundle progenitor region; *TET14* expression was restricted to the vascular progenitor strand in the cotyledons, suggesting that *TET1*, *TET4*, *TET5*, *TET10*, and *TET14* might participate in radial patterning. *TET8* was expressed in the apical domain of the heart stage embryo and in the tip regions of the cotyledons of the torpedo and mature stage embryo (Fig. 2). After germination, expression remained at the apical domains and vascular tissues: *TET3* in the SAM-organizing center

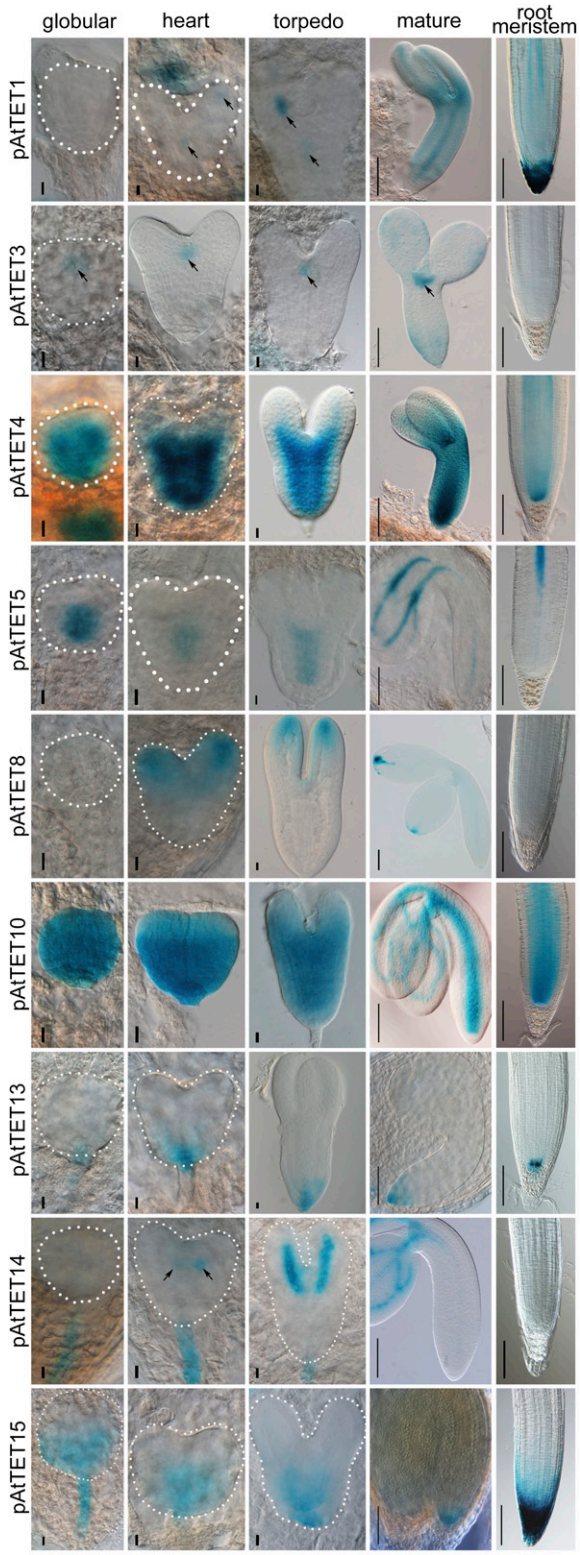

Figure 2. *TET* expression patterns during embryogenesis and in the primary root meristem after germination. Transgenic plants shown are as follows: *pAtTET1*::*NLS-GFP/GUS*, *pAtTET3*::*NLS-GFP/GUS*, *pAtTET4*::*NLS-GFP/GUS*, *pAtTET5*::*NLS-GFP/GUS*, *pAtTET8*::*NLS-GFP/GUS*, *pAtTET10*::*NLS-GFP/GUS*, *pAtTET13*::*NLS-GFP/GUS*, *pAtTET14*::*NLS-GFP/GUS*, and *pAtTET15*::*NLS-GFP/GUS*. Columns represent consecutive developmental stages: globular, heart, torpedo, and mature. Dotted lines delineate the outlines of the young embryos. Arrows in *TET1*, *TET3*, and *TET14* images indicate gene expression sites. Bars = 0.01 mm (globular, heart, and torpedo stages) and 0.1 mm (mature embryo and root meristem).

(Supplemental Fig. S1A), *TET1* and *TET15* in the lateral root cap (Fig. 2), *TET13* in the quiescent center (QC) of the primary root (Fig. 2), *TET1*, *TET5*, and *TET10* in the vascular bundle of the primary root and rosette leaves (Figs. 2 and 5, A and B; Supplemental Fig. S1C), and *TET14* in the vascular tissue of rosette leaves (Supplemental Fig. S1N).

Remarkably, *TET2* was specifically expressed after germination in the stomatal guard cell lineage during early leaf development. *TET2* expression was not detected in the meristemoid mother cell that originates from a protodermal cell, but it was in the small triangle-shaped daughter cell (called the meristemoid) generated after the first asymmetric division (Fig. 3A) and not in the large daughter cell (called the stomatal lineage ground cell). *TET2* expression remained in the guard mother cell (Fig. 3D) after the first and subsequent asymmetric divisions (Fig. 3, B and C) and in mature guard cells (Fig. 3E).

TET gene expression in progenitor tissues, domains, and cells remained in stem cells of shoot or root apical meristems or in their derived differentiated tissues or cell types in the seedling, suggesting that their function is required at different developmental stages. The variation in spatial and temporal expression patterns of the 17 *TET* genes suggests a range of functions in the plant's life cycle.

Divergent *TET* Expression Patterns within Clades, But Overlapping among Clades

The *TET* gene family consists of different clades with duplicated or triplicated members (Cnops et al., 2006; Wang et al., 2012; Boavida et al., 2013), showing diverging expression profiles (Figs. 1–3). Indeed, the duplicated genes *TET1* and *TET2* had strikingly divergent gene expression patterns. The *TET1* asymmetric gene expression pattern was found in vascular tissue precursor cells in the embryo, in the columella cells and vascular tissues of the primary root (Fig. 2), in the vascular tissues of cotyledons and rosette leaves, and in the stigma and transmitting tissue of the female gametophyte (Supplemental Figs. S1, C, J and N, and S2, A and B), which correlated with *tet1* mutant phenotypes observed in root and leaf (Cnops et al., 2000, 2006), in SAM (Chiu et al., 2007), in embryo (Lieber et al., 2011), and in fertility, which was strikingly different from *TET2* expression specifically in the stomatal cell lineage (Fig. 3). The duplicated genes *TET3* and *TET4* also had divergent expression patterns. *TET3* was expressed in the SAM precursor cells during embryogenesis (Fig. 2) and in the SAM-organizing center of the seedling (Supplemental Fig. S1A). The TET3-GFP protein moved toward and along the plasma membrane and

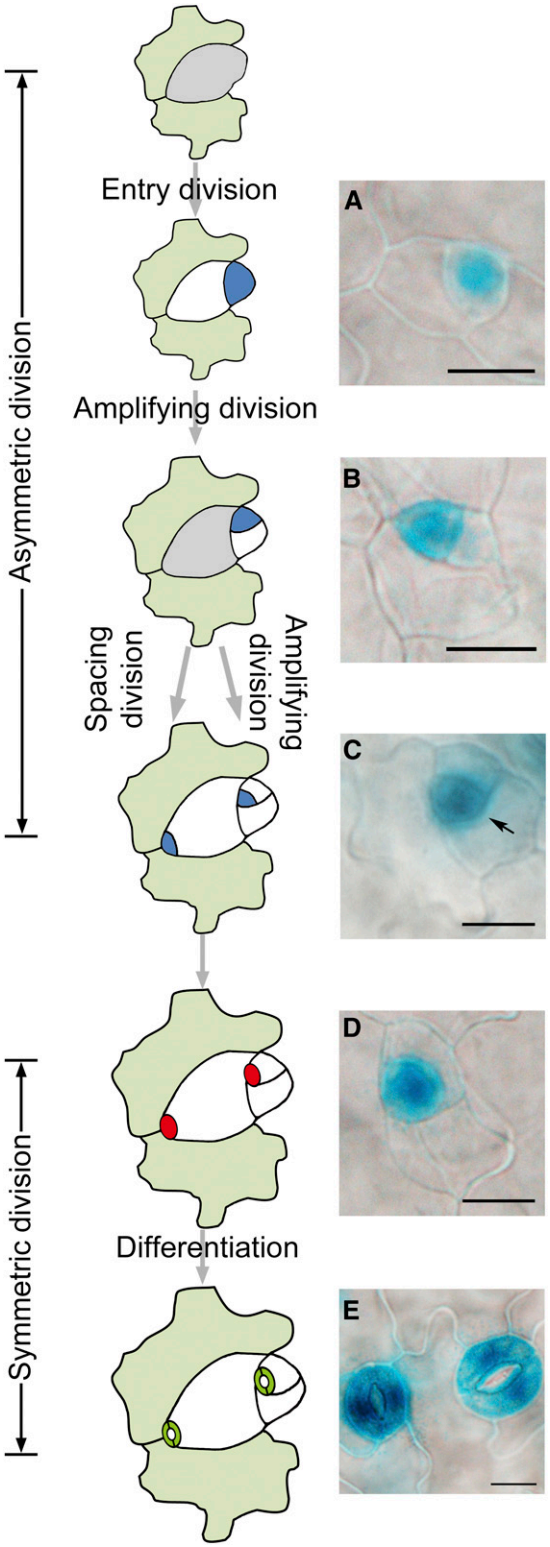

Figure 3. Diagram of Arabidopsis stomatal development (left; based on Pillitteri and Torii [2012]) and the respective *TET2* expression patterns at the abaxial epidermis of 6-d-old cotyledons of the *pAtTET2::NLS-GFP/GUS* line (right). A, *TET2* expression in the meristemoid after entry division. B and C, *TET2* expression in the meristemoid after one or two additional asymmetric divisions. The arrow indicates the meristemoid. D and E, *TET2* expression in the guard mother cell and the mature guard cells, respectively. Cells in different colors are as follows: meristemoid mother cell, gray; meristemoid, blue; stomatal lineage ground cell, white; guard mother cell, red; guard cell, green; pavement cell, light green. Bars = 0.01 mm.

localized itself at the plasmodesmata (Supplemental Fig. S1B; Supplemental Movie S1), which confirmed previous purification from the Arabidopsis plasmodesmal proteome (Fernandez-Calvino et al., 2011). In the primary root, *TET3* was expressed in the cortex, endodermis, and pericycle at the differentiation zone (Fig. 2). *TET4* was expressed in vascular tissue progenitor cells during embryonic development, in the QC and vascular tissue of the primary root (Fig. 2), in stomatal guard cells of cotyledons and anthers, and in the basal region of the flower (Supplemental Figs. S1E and S2A). Similarly, the triplicated genes *TET7*, *TET8*, and *TET9* had distinct expression patterns. *TET7* expression was restricted to the pollen (Supplemental Fig. S2C). *TET8* was expressed in the apical domain of the embryo, starting from the heart stage (Fig. 2), in the differentiation zone of the primary root (Fig. 2), and in stipules and hydathodes of rosette leaves (Supplemental Fig. S1, F and G). *TET9* was expressed in the vascular tissues of the primary root (Fig. 2), in cotyledons and rosette leaves, in the SAM, and in trichomes and surrounding pavement cells (Supplemental Fig. S1, J–L). *TET10* is the only single gene within the family. It was widely expressed in globular, heart, and torpedo stages during embryogenesis (Fig. 2). In the mature embryo, it was expressed in the vascular tissue of root and cotyledons. After germination, the expression remained in the primary root meristem but not in the vascular tissue of cotyledons (Fig. 2). *TET11* was expressed only in the pollen (Supplemental Fig. S2C), and its duplicated gene, *TET12*, was expressed in the primary root and stipules (Supplemental Fig. S1M), suggesting a thoroughly diverged function. The triplicated genes *TET13*, *TET14*, and *TET15* diverged in expression patterns. *TET13* was expressed in the embryonal hypophysis, in the QC, stem cells, and columella cells of the primary root, and in the lateral root primordia (LRP; Figs. 2 and 4, A and E–N). *TET14* expression was restricted to vascular precursor cells of heart stage embryos and in the cotyledonary vascular tissues of the mature embryo (Fig. 2). *TET15* was expressed in the basal domain of the heart stage embryo, in the lateral root cap and columella cells (Fig. 2), in the pollen tubes, and in stomatal guard cells of sepals (Supplemental Fig. S2, B and C). *TET16* was expressed only in the basal region of the flower and pollen (Supplemental Fig. S2C), and no *TET17* gene expression was detected in any of the organs, which was consistent with the absence of gene expression in transcriptome data of Genevestigator or the eFP browser throughout development. Nevertheless, nucleus-localized TET17-GFP protein was detected in mature pollen (Boavida et al., 2013).

However, overlapping expression patterns were observed in *TET* genes of different clades in pollen (*TET1*,

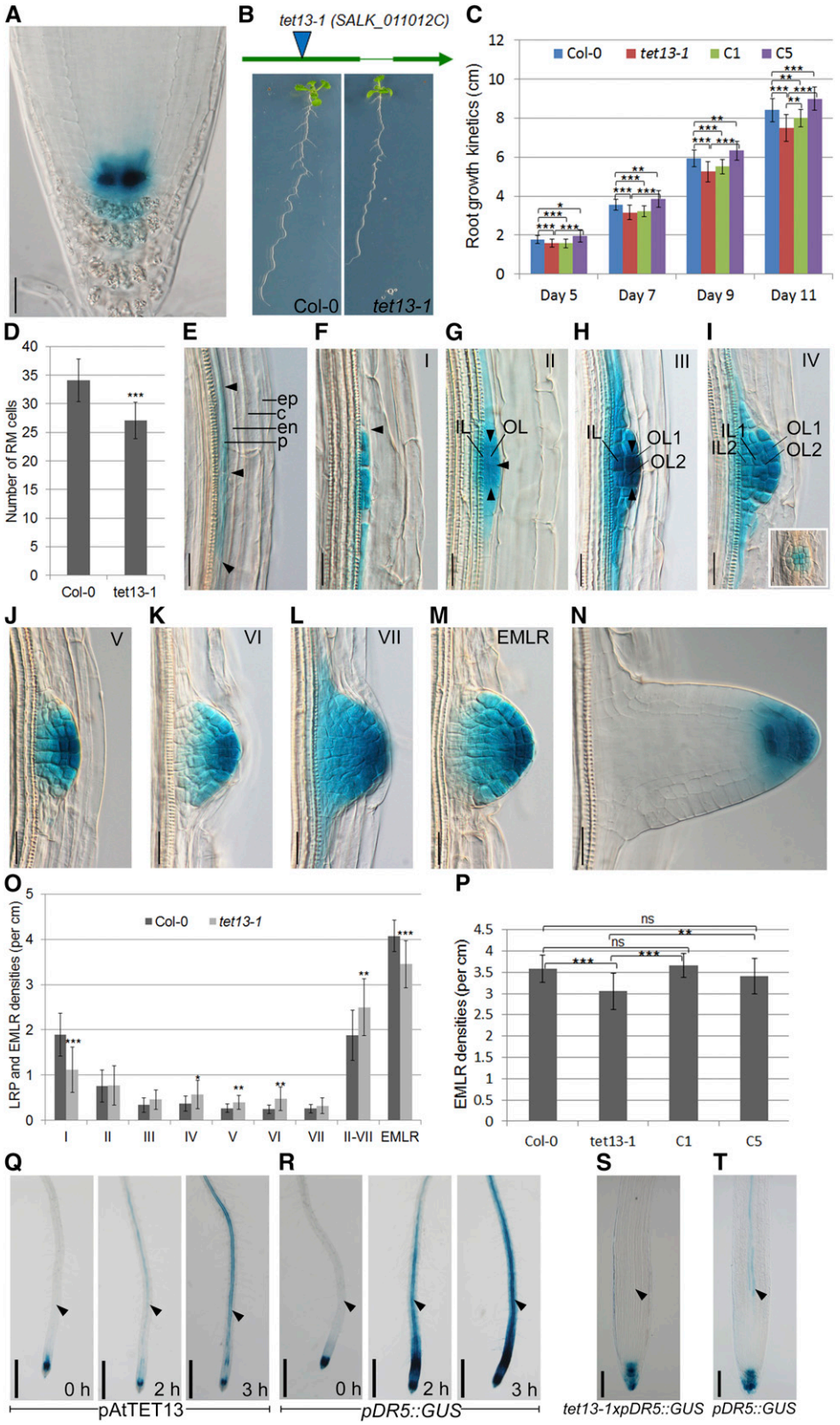

Figure 4. *TET13* expression in the primary root and LRP, *tet13-1* root phenotypes, and complementation. Transgenic plants shown are as follows: *pAtTET13*::*NLS-GFP/GUS* (A, E–N, and Q), *tet13-1* (B–D, O, and P), C1 and C5 (*tet13-1* containing one and two T-DNA loci with *p35S*::*TET13*; C and P), *pDR5*::*GUS* (R and T), and *tet13-1* × *pDR5*::*GUS* (S). A, *TET13* expression in the primary root tip. B, *tet13-1* scheme and 12-d-old seedlings of Columbia-0 (Col-0) and *tet13-1* growing vertically under the 24-h light condition. C, Primary root growth kinetics. Means ± SD are presented (n = 22–33). Asterisks mark significant differences: *, $P < 0.05$; **, $P < 0.01$; and ***, $P < 0.001$. D, Root meristem size (defined as the number of root meristem [RM] cells) of 6-d-old seedlings. Means ± SD are presented (n = 28–39). E to N, Detailed expression analysis of *TET13* at different stages during lateral root development. Corresponding developmental stages I to VII and emerged lateral root (EMLR) are indicated in the top right corner. IL and OL, Inner and outer layers, respectively; c, cortex; en, endodermis; ep, epidermis; p, pericycle. Arrowheads indicate the division planes. The inset in I shows the top view of stage IV. O, Staging of LRP and EMLR densities. Means ± SD are presented (n = 20). P, EMLR densities. Means ± SD are presented (n = 22–33). ns, Not significant. Asterisks mark significant differences: *, $P < 0.05$; **, $P < 0.01$; and ***, $P < 0.001$. Q and R, NAA-induced *TET13* (Q) and *pDR5*::*GUS* (R) expression. The seedlings were grown on 10 μM NPA medium for 72 h after germination and then transferred to 10 μM NAA medium for 0, 2, and 3 h. S and T, *DR5*::*GUS* expression patterns at the root basal meristem in 7-d-old *tet13-1* × *pDR5*::*GUS* (S) and wild-type (T) seedlings. In Q to T, black arrowheads indicate sites of inducible expression. Bars = 0.01 mm (E–N), 0.1 mm (S and T), and 0.5 mm (Q and R).

TET2, *TET3*, *TET4*, *TET7*, *TET8*, *TET9*, *TET10*, *TET11*, *TET13*, *TET14*, *TET15*, and *TET16*; Supplemental Fig. S2C) and in vascular tissues of the embryo and/or the seedling (*TET1*, *TET3*, *TET4*, *TET5*, *TET6*, *TET8*, *TET9*, *TET10*, *TET12*, and *TET14*; Fig. 2; Supplemental Fig. S1), suggesting redundancy in function that might complicate functional analysis by the mutational approach. Transfer DNA (T-DNA) insertion lines in *TET* genes were characterized as knockout or knockdown alleles by quantitative reverse transcription-PCR, and phenotyping in the respective mutants was done with particular attention to organs in which the respective *TET* gene was expressed. Strikingly, only in the *TET13* knockout line, *tet13-1*, was a clear phenotype observed in the primary and lateral root development, which correlated with its site of expression (Supplemental Table S1). Although the single mutant analysis was not exhaustive for putative phenotypes, the identification of a phenotype for only one *TET* gene argued for functional redundancy among the other *TET* genes and showed the need for double and triple mutant combinations.

TET13 Function in Primary Root Growth and Lateral Root Development

TET13 expression and mutant phenotypes were studied in more detail during primary and lateral root development. Arabidopsis root identity is specified early during embryogenesis. The cells at the basal region of the globular embryo will give rise to the hypocotyl, primary root, and root stem cells. The lens-shaped cells in this region are the progenitors of the QC, which is crucial for maintaining root stem cell identity (van den Berg et al., 1997). In wild-type plants, the stem cells surrounding the QC are maintained in the undifferentiated state. In the primary root, *TET13* was predominantly detected in the QC, most of the stem cells (cortex/endodermis initials, pericycle initials, vascular tissue initials, and columella initials but not epidermis initials), the first two columella cell layers, and the two middle cells in the root cap (Fig. 4A). *TET13* promoter activity was equally present at the two QC cells of 35 seedlings, indicating that *TET13* was not cell cycle regulated. The function of *TET13* in primary root and lateral root development was studied in the T-DNA insertion line *tet13-1* (SALK_011012C), in which the T-DNA is located at the first exon, resulting in a gene knockout (Boavida et al., 2013). In addition, complementation of root phenotypes was studied in the C1 and C5 complementation lines of *tet13-1* containing one and two T-DNA loci with *p35S*::*TET13*, respectively. The primary root length was reduced significantly in *tet13-1* (Fig. 4, B and C), partially restored to wild type in the C1 line, and fully restored and even larger than the wild type in the C5 line (Fig. 4C). The primary root length is determined by several parameters such as meristem, elongation zone, and differentiation zone size and cell length at these zones. The meristem size, defined as the number of cells from the QC to the first elongated cell in the cortex cell file (Casamitjana-Martínez et al., 2003) was reduced significantly in *tet13-1* (27 ± 3 [SD] cells) as compared with the wild type (34 ± 4 cells; Fig. 4D; Supplemental Fig. S3A). Below the QC, there are one or two layers of undifferentiated columella initials that generate the differentiated columella cells containing starch that stains purple by Lugol solution. One of the functions of the QC is to keep the surrounding initials in an undifferentiated state, because defective QC function results in a differentiated cell layer below the QC instead of the columella initial cell layer (van den Berg et al., 1997; Sarkar et al., 2007). Exogenous auxin (1-naphthaleneacetic acid [NAA]) or auxin transport inhibitor (*N*-1-naphthylphthalamic acid [NPA]) promoted the differentiation of columella initial cells in wild-type seedlings but not in mutants in auxin biosynthesis or transport (Ding and Friml, 2010). In *tet13-1* mutants, one or two columella initial cell layers were measured in primary roots, which is comparable with the wild type, and no precocious differentiation of the columella initials was observed (Supplemental Fig. S3, B and C); hence, columella initial cell identity was maintained in the *tet13-1* mutant under normal conditions and after NAA and NPA treatment (Supplemental Fig. S3, D–F). The architecture of the QC and initials was normal in the *tet13-1* mutant, as visualized by confocal microscopy with propidium iodide staining (Supplemental Fig. S3G), indicating no function of *TET13* in cytokinesis. *tet13-1* seedlings were equally insensitive as wild-type seedlings to hydroxyurea, a replication-blocking agent, because no dead cells were observed after propidium iodide staining (Supplemental Fig. S3, H and I).

Auxin oscillation in the pericycle of the primary root basal meristem (De Smet et al., 2007) determines the lateral root founder cell fate, and their anticlinal asymmetric division results in a single-layered primordium composed of small daughter cells flanked by two large daughter cells, termed stage I. During lateral root development, *TET13* was active at the two neighboring pericycle cells before the asymmetric division (Fig. 4E). At stage I, the expression was stronger in the two newly generated, small daughter cells (Fig. 4F). From stage II to VII (Fig. 4, G–L), anticlinal and periclinal divisions form a dome-shaped primordium with two to seven cell layers. At stage II, *TET13* was expressed equally strongly in the tip cells at the outer layer as well as in the middle two cells at the inner layer (Fig. 4G). From stage III on, *TET13* expression was always stronger in the tip cells at the outer layer (Fig. 4, H–M) and comparable to that of the *pDR5*::*GUS* reporter gene (Benková et al., 2003). At stage VIII, upon lateral root emergence, *TET13* was expressed in the QC and columella (Fig. 4N).

Lateral root initiation stages and lateral root emergence were analyzed in *tet13-1* mutants: the number of stage I LRP was reduced severely (Fig. 4O), which correlated with early *TET13* expression in the pericycle founder cells before the first asymmetric division (Fig. 4E); stage IV, V, and VI LRP densities were increased significantly, whereas the number of stage II, III, and VII LRP was increased slightly in *tet13-1* (Fig. 4O); the EMLR density was reduced significantly (Fig. 4, O and P).

Because the LRP and EMLR densities, defined as the number of LRP and EMLRs per 1 cm of primary root, were significantly increased and reduced, respectively (Fig. 4O), *TET13* has a potential role in restricting lateral root initiation and promoting lateral root emergence. The EMLR density in the complementation lines C1 and C5 was restored to the wild-type level (Fig. 4P). In an assay for synchronous lateral root initiation (Himanen et al., 2002), seedlings were first incubated on medium containing the auxin transport inhibitor NPA and then transferred to NAA medium, after which synchronous lateral root initiation was monitored. The *TET13* promoter activity was induced after 2 h of NAA induction at the xylem pole of the pericycle, which coincides with the onset of stage I (Fig. 4Q); after 3 h of NAA induction, two clear blue lines marked the pericycle (Fig. 4Q), which was similar to the *pDR5*::*GUS* reporter gene expression pattern (Fig. 4R), indicating that *TET13* expression is auxin inducible and specific for pericycle cells. In the *tet13-1* mutant, the *pDR5*::*GUS* reporter gene was not or very weakly expressed at the basal meristem in eight out of 13 tested seedlings (Fig. 4S), whereas in all 11 wild-type seedlings it was expressed (Fig. 4T), indicating that auxin accumulation in the pericycle founder cells is affected. Hence, the *tet13-1* mutant allele and the complementation lines showed that TET13 has a function in the primary root affecting apical meristem size and root length and in lateral root initiation and emergence, which is consistent with its expression sites in the root.

TET5 and *TET6* Have Redundant Functions in Root and Leaf Growth

TET5 and *TET6* were the only duplicated genes with similar expression patterns (i.e. in the vascular tissue of all organs, except for embryos, in which only *TET5* was expressed; Fig. 1). At the globular stage, *TET5* expression was restricted to the vascular tissue progenitor cells (Fig. 1). After germination, both *TET5* and *TET6* were expressed in the pericycle, the vascular tissues of the primary root starting from the transition zone, the hypocotyl, cotyledons, and rosette leaves (Fig. 5, A and B). Transverse sections of the primary root showed that, at the meristem-elongation transition zone, *TET5* and *TET6* were expressed in the phloem, a few procambial cells surrounding the phloem, and the phloem-pole pericycle but not in the protoxylem (Fig. 5A, bottom). At the differentiation zone, they were expressed in the pericycle and all vascular tissues except for the protoxylem (Fig. 5A, top). In the siliques, they were expressed in the funiculus, which has a function in guiding the pollen tube to reach the micropyle during fertilization (Supplemental Fig. S2B). The redundant expression patterns suggest redundant functions, which was confirmed by single and double mutant analyses. Several *tet5* and *tet6* mutant alleles were analyzed for their *TET5* and *TET6* gene expression: *tet5-1* (GABI-Kat 290A02, insert in promoter), *tet5-2* (SALK_148216, insert in first exon; Boavida et al., 2013), and *tet5-3* (SALK_020009C, insert in second exon) are *TET5* knockouts, *tet6-1* (SALK_005482C, insert in promoter) is a *TET6* up-regulated line, and *tet6-2* (SALK_139305, insert in promoter) is a *TET6* knockdown (Fig. 5C). No morphological alterations or patterning defects were observed in the roots, leaves, or inflorescences of the single mutants *tet5-1*, *tet5-2*, *tet5-3*, and *tet6-2*. However, morphological analysis of three different double mutant combinations, *tet6-2tet5-1* (Supplemental Fig. S4), *tet5-2tet6-2* (Supplemental Fig. S4), and *tet5-3tet6-2* (Fig. 5, E–I), revealed synergistic phenotypes, such as an enlarged leaf size in seedlings at all stages of rosette development (Fig. 5F) due to a significantly increased total number of cells per leaf (23,238 ± 2,967 in *tet5-3tet6-2* compared with 15,495 ± 1,635 in *tet5-3* and 15,197 ± 2,887 in *tet6-2*; Fig. 5G), increased fresh weight in 21-d-old seedlings (Fig. 5H), and longer primary roots in a root growth kinetic study (Fig. 5I), confirming redundant functions of *TET5* and *TET6* in restricting cell proliferation during root and leaf growth.

TET Promoter cis-Regulatory Elements to Predict Responses to Environmental and Developmental Stimuli

The cis-regulatory elements (or motifs) were identified in the *TET* promoter regions using an integrative bioinformatics approach (see "Materials and Methods") in order to further study and explain the divergence, overlap, and redundancy in *TET* gene expression. The cis-regulatory elements also provided information about environmental and developmental stimuli that might influence *TET* gene expression, which could be used for further functional analysis. Apart from mapping known cis-regulatory elements to the 2-kb promoters of the different *TET* genes, also coregulatory genes, evolutionary sequence conservation, and information about open chromatin regions (DNaseI-hypersensitive [DH] sites) were integrated to identify cis-regulatory elements and TFs putatively regulating *TET* genes. Recently, we have shown that combining complementary regulatory data sources has a positive impact on reducing the high number of false positives associated with simple mapping of cis-regulatory elements and strongly increases the likelihood that retained regulatory interactions are biologically functional (Vandepoele et al., 2009; Van de Velde et al., 2014). To identify *TET* cis-regulatory elements shared with coregulated genes, for each *TET* gene, Genevestigator was first used to identify a set of tissue and perturbation experiments in which the gene was strongly responsive (see "Materials and Methods"). Next, coregulated genes were identified under these conditions, and enrichment analysis was performed to identify cis-regulatory elements significantly shared between each *TET* gene and its coregulated genes, considering the motifs obtained by simple motif mapping or simple motif mapping filtered for DH sites or filtered for evolutionary conservation (indicated with analysis type motif, DH, and CM in Supplemental Table S2, respectively). In total, 128 cis-regulatory elements were identified in the *TET*

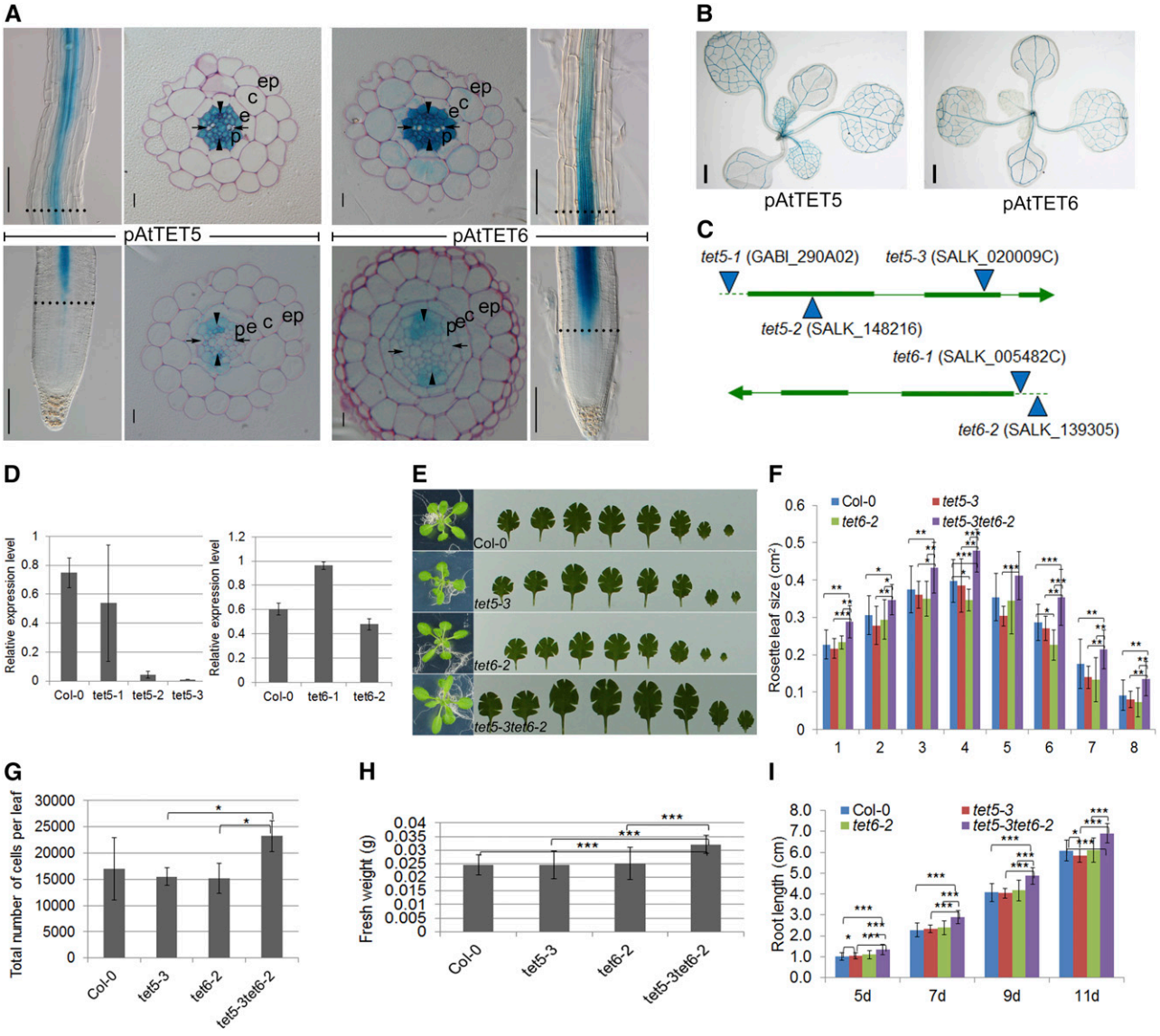

Figure 5. *TET5* and *TET6* expression, and *tet5-3*, *tet6-2*, and *tet5-3tet6-2* mutant phenotypes. Transgenic plants shown are as follows: *pAtTET5*::*NLS-GFP/GUS* (A and B), *pAtTET6*::*NLS-GFP/GUS* (A and B), *tet5-3* (C–I), *tet6-2* (C–I), and *tet5-3tet6-2* (E–I). A, *TET5* and *TET6* expression in the vascular tissue of the meristem-elongation transition zone (between dashed lines) and the differentiation zone (top) of the primary root, of which part of the elongation zone is omitted; the root tip (lower images) and the differentiation zone (upper images) are shown. Transverse sections show the transition zone and differentiation zone, as indicated by the dashed lines. c, Cortex; e, endodermis; ep, epidermis; p, pericycle. Arrowheads and arrows indicate phloem pole and protoxylem, respectively. B, *TET5* and *TET6* expression in the rosette leaves. C, *TET5* and *TET6* schemes with T-DNA insertions. Thick, thin, and broken lines indicate exons, introns, and promoter, respectively. D, Relative *TET5* (right) and *TET6* (left) transcript levels in 7-d-old seedlings measured by quantitative reverse transcription-PCR. Means ± SD are presented ($n = 3$). E, Rosette and leaf series of 21-d-old seedlings. From left to right are leaf 1 to leaf 8; incisions were made to make the leaves fully expanded when necessary. F, Quantification of the rosette leaf sizes in E. Means ± SD are presented ($n = 8$–10). G, Total number of cells per leaf. Leaf 1 and/or 2 were used. Means ± SD are presented ($n = 3$). H, Fresh weight of 21-d-old seedlings. Only rosette leaves were used for the experiment. I, Primary root growth kinetics (root length). Means ± SD are presented ($n = 31$–39). Asterisks in all graphs mark significant differences: *, $P < 0.05$; **, $P < 0.01$; and ***, $P < 0.001$. Bars = 0.01 mm (A, transverse section), 0.1 mm (A, longitudinal section), and 1 mm (B).

promoters and their respective coregulated genes, yielding regulatory information about 13 *TET* genes (no result for *TET11*, *TET13*, *TET16*, and *TET17*). More than half of the regulatory elements (71 of 128) were identified through the enrichment analysis using the motif-mapping files filtered for DH sites or evolutionary conservation, indicating that they are functionally related to accessible TF-binding sites in open chromatin regions or to regulatory elements that have been conserved during hundreds of millions of years of evolution (Supplemental Table S2).

A heat map was generated with *TET* differential gene expression upon a selection of perturbations in Genevestigator (Supplemental Fig. S5A) and used to verify the cis-regulatory elements in *TET* promoters identified in Supplemental Table S2. The cis-regulatory elements identified from *TET1*, *TET2*, *TET3*, *TET4*, *TET5*, *TET6*, *TET8*, *TET9*, and *TET16* correlated with their expression patterns or inducible conditions. *TET1* up-regulation by high light correlates with the enrichment in the light-regulated gene-binding sites and induction upon brassinolide treatment with a GATA promoter motif (Supplemental Table S2) that can be recognized by GATA family TFs, some of which mediate the cross talk between brassinosteroid and light signaling pathways (Luo et al., 2010). *TET2* promoter elements are related mainly to stress responses, including cold, dehydration, and drought responses (Supplemental Table S2), and fit with the up-regulation of *TET2* in response to abscisic acid (ABA), cold, and drought (Supplemental Fig. S5A), which can induce stomatal closure. *TET2* function in the mature stomatal guard cell might relate to stomatal closure caused by stress conditions. *TET3* up-regulation by ABA, cold, and drought and in the *C-REPEAT/DEHYDRATION-RESPONSIVE ELEMENT-BINDING FACTOR3* (*CBF3*) overexpression background (Supplemental Fig. S4A) correlates with cold- and drought-responsive elements and the CBFHB element that is the binding site of *CBF3* (Supplemental Table S2), a TF involved in cold response. The *TET3* expression pattern in the SAM and the cold response element at the promoter region suggest a function in cold sensing at the SAM or upon floral transition. *TET4* is also up-regulated by ABA, cold, and drought and in the *CBF3* overexpression background (Supplemental Fig. S5A) and correlates with ABA response elements and elements in seed-specific promoters (Supplemental Table S2; Ezcurra et al., 2000; Chandrasekharan et al., 2003). *TET5* and *TET6*, both expressed in the vascular tissue, contain distinct sugar response promoter elements that suggest a role in sugar sensing and growth (Supplemental Table S2). *TET8* and *TET9* promoter regions contain defense and pathogen response elements (Supplemental Table S2), which correlate with high up-regulation by pathogens and elicitors (Supplemental Fig. S5A); in addition, there are three endosperm-specific elements that fit with *TET8* expression in the endosperm (Supplemental Table S2; Supplemental Fig. S1H). One of them is the MYB98-binding site; *MYB98* expression is observed in the synergid cells (Kasahara et al., 2005). Presumably, *TET8* is expressed in the synergid cells as well (Supplemental Fig. S1I). *TET16* is 63 times up-regulated during pollen tube growth (Supplemental Fig. S5A) and is expressed specifically in pollen (Supplemental Fig. S2C), suggesting a function in this process.

In conclusion, the cis-regulatory element analysis confirmed the divergence in reporter expression of duplicated *TET* genes. The presence of the same regulatory elements in *TET* genes of different clades, such as the root-specific element in *TET4* and *TET10* and the vascular tissue-specific element in *TET4*, *TET8*, *TET9*, and *TET12* (Supplemental Table S2), supported the redundancy of the reporter expression of *TET* genes over the different clades.

A TF-*TET* Gene Regulatory Network to Predict Function in Molecular Pathways

In order to obtain a better understanding of the transcriptional regulation of *TETs* and their positions in molecular pathways, a TF-*TET* gene regulatory network was built by combining different regulatory data sets. Apart from conserved TF-binding sites, also chromatin immunoprecipitation (ChIP) TF-binding data and TF expression perturbation information were integrated to generate a TF-*TET* gene regulatory network (data types denoted as conserved motif, ChIP, and DE in Fig. 6, respectively). Although these data sets cover different aspects of gene regulation, it is important to note that the obtained gene regulatory network offers only a partial view of *TET* regulation, since, as for many Arabidopsis TFs, no binding site information or experimental data are available.

The conservation of cis-regulatory elements has been used to delineate gene regulatory networks in different species (Aerts, 2012), and a recent study in Arabidopsis used a phylogenetic footprinting approach to delineate conserved gene regulatory networks based on known binding sites for 157 TFs (Van de Velde et al., 2014). TF ChIP-Seq and ChIP-chip analyses have been used to identify target genes of different plant regulators, including TFs involved in flowering, circadian rhythm and light signaling, cell cycle, and hormone signaling (Mejia-Guerra et al., 2012). To integrate experimental ChIP TF-binding information, the network of Heyndrickx et al. (2014) was used, in which 27 publicly available TF-ChIP data sets have been reprocessed through an analysis pipeline consisting of quality control, platform-specific signal processing, and peak calling to generate TF-*TET* gene interactions. Next to the physical binding of a TF in the vicinity of a *TET* gene, which can serve as a proxy for *TET* gene regulation, information about the regulation of a *TET* gene by a specific TF was also taken into account. Therefore, we screened differentially expressed genes that were obtained through transcript profiling after perturbation (knockout or overexpression) of the normal activity of a TF from 15 publicly available studies. Differentially expressed genes from five studies, in which regulatory information about *TET* genes was reported, were retained, complementing the ChIP binding data for AGL15, BES1, LFY, and FUS3 (see "Materials and Methods"). Most of the *TETs* were regulated by multiple TFs (i.e. *TET3*, *TET4*, *TET8*, *TET9*, and *TET14*). Some duplicated *TETs* shared common TFs (i.e. *TET3* and *TET4*, *TET5* and *TET6*, and *TET8* and *TET9*; Fig. 6).

To further validate regulatory interactions in the network, such as those inferred through ChIP and conserved TF-binding sites, expression perturbation data from Genevestigator were obtained for nine TFs

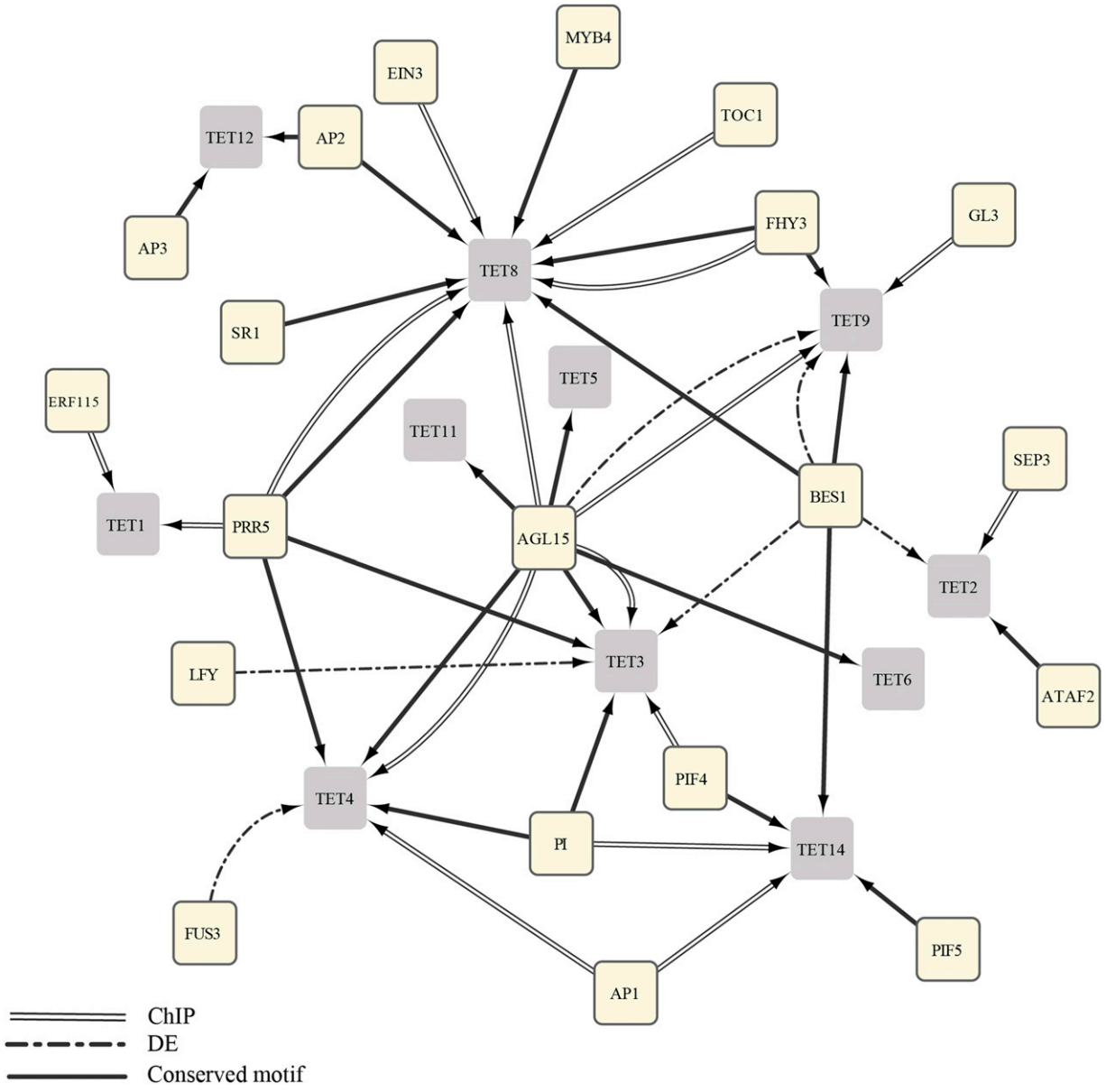

Figure 6. TF-*TET* gene regulatory network. Nodes and arrows depict genes and regulatory interactions, and yellow and gray rounded rectangles are TFs and *TETs*, respectively. The arrows do not represent any positive or negative regulation between the TFs and *TETs*. Regulation identified by ChIP sequencing and a conserved binding motif are shown with doubled lines and solid lines, respectively. Differentially expressed (DE) regulation is shown with dashed lines. AGL15, AGAMOUS-LIKE15; AP, APETALA; ATAF2, ARABIDOPSIS NAC DOMAIN-CONTAINING PROTEIN81; BES1, ethyl methanesulfonate-mutagenized allele of BRASSINOSTEROID INSENSITIVE1-SUPPRESSOR1; EIN3, ETHYLENE-INSENSITIVE3; ERF115, ETHYLENE RESPONSE FACTOR115; FHY3, FAR-RED ELONGATED HYPOCOTYLS3; GL3, GLABRA3; LFY, LEAFY; MYB4, MYB DOMAIN PROTEIN4; PI, PISTILLATA; PIF, PHYTOCHROME-INTERACTING FACTOR; PRR5, PSEUDO-RESPONSE REGULATOR5; SEP3, SEPALLATA3; SR1/CAMTA3, SIGNAL RESPONSIVE1/CALMODULIN-BINDING TRANSCRIPTION ACTIVATOR3; and TOC1, TIMING OF CHLOROPHYLL A/B-BINDING PROTEIN EXPRESSION1.

(AGL15, AP1, PI, EIN3, LFY, PIF4, PIF5, TOC1, and SR1) and TF-*TET* interactions were confirmed by significant differential expression after TF perturbation (Table I). The TFs in the regulatory networks were related to light response (PIF4 and PIF5), circadian clock (TOC1), floral organ identity (AP1, AP2, AP3, SEP3, and PI), flowering initiation (AGL15 and LFY), and defense response (EIN3, MYB4, and SR1) and identify the respective *TET* genes as novel components of specific developmental or physiological pathways.

DISCUSSION

Arabidopsis *TET* genes are expressed in different organs/tissues and cell types during embryonic and

Table I. *TET transcript changes upon TF perturbation*

Genevestigator microarray studies on genotypes perturbed for the TFs identified in Figure 6 were analyzed for differential *TET* transcript levels at $P < 0.05$. In double mutant and artificial microRNA backgrounds, only the TFs of interest are listed. Fold change was calculated from the $\log_2$ ratio. DE, Differentially expressed. − and + represent down-regulation and up-regulation, respectively. Asterisks indicate data that were obtained from the same studies in Figure 6.

Genotype	DE TF	Fold Change, DE TF	*P*	DE *TET*	Fold Change, DE *TET*	*P*
agl15-4agl18-1/Col-0*	*AGL15*	−3.77	<0.001	*TET3*	+1.35	0.03
				TET4	+1.66	<0.001
				TET5	+1.17	0.207
				TET6	+1.33	0.039
				TET8	+1.80	0.019
				TET9	+2.17	<0.001
				TET11	+1.18	0.107
35S::amiR-mads-2(MIR319a)_strong/Col-0	*AP1*	−5.24	<0.001	*TET4*	−1.18	0.051
				TET14	−1.04	0.71
	PI	−1.95	0.004	*TET3*	−1.77	0.054
				TET4	−1.18	0.051
				TET14	−1.04	0.71
ein3-1eil1-1/coi1-2	*EIN3*	−9.53	0.003	*TET8*	−1.40	0.049
35S:LFY-GR/Landsberg *erecta*	*LFY*	+36.58	<0.001	*TET3*	−1.19	0.002
lfy-12/Col-0* (shoot apex, rosette is 50% of final size)	*LFY*	−3.33	0.007	*TET3*	+1.63	0.006
lfy-12/Col-0* (inflorescence, first flower open)	*LFY*	−1.82	0.006	*TET3*	+1.80	0.018
pif4-101pif5-3/Col-0	*PIF4, PIF5*	−1.04, −70.1	0.746, <0.001	*TET3*	−1.28	0.008
				TET14	+1.24	0.064
Alc::TOC1/Col-0	*TOC1*	+8.59	<0.001	*TET8*	−1.17	0.013
camta3-2/Col-0	*SR1*	−5.61	0.003	*TET8*	+1.88	0.027

vegetative development. Intriguingly, the onset of expression coincided with the onset of patterning and cell specification in globular and heart stage embryos (*TET1*, *TET3*, *TET4*, *TET5*, *TET8*, *TET10*, *TET13*, *TET14*, and *TET15*) and in seedlings at the initiation of the stomatal cell lineage (*TET2*) or at the asymmetric division in the primary root pericycle upon lateral root initiation (*TET13*), which suggests a role for these *TET* genes in cell specification. Plant cells are surrounded by a rigid but dynamic cell wall, which prevents them from migration during specification; hence, they acquire their fate by positional information from neighboring cells. The cellular communication involves diffusible or actively transported molecules, such as peptides, small RNAs, TFs, or phytohormones, that upon recognition by competent cells trigger signaling cascades that result in the initiation or repression of specific developmental programs (Sparks et al., 2013). Remarkably, nine *TETRASPANINs* (*TET1*, *TET3*, *TET4*, *TET5*, *TET8*, *TET10*, *TET13*, *TET14*, and *TET15*) are expressed in embryonic progenitor tissue, and three are expressed early in the cell lineage of the seedling until differentiation (*TET2*, *TET9*, and *TET13*). The expression in the progenitor cells of a cell lineage suggests that they might be required in progenitor cell identity establishment or maintenance or in the lateral inhibition of neighboring cells. Their expression later in the differentiated cells of the same cell lineage suggests a function in the physiology or biochemistry of the mature cells, which might be related or not to its early function. Hence, the expression of certain *TET* genes in plants, very early in a cell lineage until the differentiated state, might indicate dynamic interactions in time with partner proteins that are components of different molecular pathways.

Most of the duplicated *TET* genes have diverged expression patterns during the plant's life cycle, as was demonstrated in the *pTET*-reporter lines, and coincided with different regulatory elements in their promoters (Supplemental Table S2). Even though the duplicated *TET5* and *TET6* genes showed redundant expression in vascular tissue, different regulatory elements related to sugar sensing were identified in their promoters (Supplemental Table S2). Largely overlapping expression patterns were observed in *TET* genes over the clades in embryos, primary roots, rosette leaves, and pollen and might refer to the conservation of ancestral *TET* gene functions in specific tissues or cells. Indeed, similar regulatory elements were identified in *TET* promoters belonging to different clades, such as ABA-responsive, root-specific, and light-related motifs, which add to the putative overlap in function (Supplemental Table S2). Here, it might be more logical to suggest that these paralogous *TET* genes evolved in their promoter through subfunctionalization (Moore and Purugganan, 2005).

These overlaps might explain the mild or undetectable phenotypes in single mutants in our mutational analysis (Supplemental Table S1) and demonstrate the need for making double or triple mutant combinations over the clades to detect phenotypes. Such a strategy was rewarding in animals, resulting in strong phenotypes in mice and *D. melanogaster* (Fradkin et al., 2002; Rubinstein et al., 2006).

TET5 and *TET6* duplicated genes have the same promoter activity pattern in postembryonic vascular tissues and in cells surrounding procambial cells and the phloem, suggesting a putative redundant function in vascular bundle activity, such as in nutrient or photoassimilate transport, rather than in patterning, because no venation patterning defect was observed in the double *tet5tet6* mutant. Combining the single *tet5* and *tet6* mutants resulted in significantly enhanced growth by cell proliferation in root and shoot, suggesting that TET5 and TET6 restrict growth through a sugar-sensing mechanism, because such cis-regulatory elements were identified in their promoters (Supplemental Table S2). Indeed, Suc promotes cell proliferation by activating the cell cycle (Riou-Khamlichi et al., 2000). Arabidopsis tetraspanins can form homodimers and heterodimers when expressed in yeast (Boavida et al., 2013). The redundant function of TET5 and TET6 suggests that, for proper activity, heterodimers might need to be formed or interaction with a common protein might be required, which needs further testing.

TET13 expression in the pericycle founder cells and the gradual spatial pattern in the LRP resemble auxin accumulation and gradients that regulate lateral root development (Benková et al., 2003). *TET13* shows overlapping expression in the pericycle with *TET3*, *TET4*, *TET5*, *TET6*, *TET8*, *TET9*, *TET10*, and *TET12*, which might explain the mild phenotype in lateral root development in *tet13-1*. Significant reduction of stage I LRP density in *tet13-1* indicates that lateral root initiation is affected, and *TET13* is required to promote lateral root initiation. It nicely correlated with *TET13*-specific expression in the two pericycle founder cells before the asymmetric divisions that precede lateral root initiation and with its early inducible expression in the xylem pole pericycle at the root basal meristem upon NAA treatment (Himanen et al., 2002). Significant increase of stage II to VII LRP densities but reduced EMLR density indicate that the emergence of the lateral root is also affected in *tet13-1*, a process that is highly regulated by the transcellular auxin-dependent signaling pathway that results in cell wall remodeling in the adjacent endodermal, cortical, and epidermal cells overlaying the primordium (Swarup et al., 2008). Thus, *TET13* regulates two different aspects of lateral root development, restricting lateral root initiation and promoting lateral root emergence.

Meta-analysis of gene responses to certain perturbations gives a general idea about the gene function in biological processes. However, these responses, as measured through differential expression, could be due to indirect or secondary regulation. The regulatory elements residing in the promoter regions are primarily responsible for the gene response to the perturbations, because they are the binding sites for the TFs that regulate gene expression. The identification of upstream TFs that bind to these regulatory elements together with other regulatory data sets complemented the inference of *TET* gene functions and allowed us to position *TET* genes in specific regulatory networks describing flowering time, circadian clock, and defense response. Integration of the different expression and regulatory analyses presented in this work suggests a function for *TET3* in flowering response under low temperature. Indeed, *TET3* is expressed in the SAM-organizing center progenitor cells in embryos that remain in the seedling. Cold and dehydration response elements are enriched in the *TET3* promoter that correlate with the up-regulation of *TET3* gene expression by ABA, cold, and drought treatment. The PRR5, AGL15, and PIF4 TFs that regulate *TET3* (Fig. 6) have a function in flowering response (Adamczyk et al., 2007; Nakamichi et al., 2007; Kumar et al., 2012), and in the TF genetic perturbation backgrounds, *AGL15* and *LFY* expression levels are negatively correlated with *TET3* (Table I). Thus, the meta-analysis is hypothesis generating and will be helpful for experimental design in further functional analyses. Our analyses suggest a function for *TET8* in the defense response. The *TET8* gene is up-regulated upon pathogen treatment, which correlated with the enrichment of defense response cis-regulatory elements in its promoter. The SR1/CAMTA3, MYB4, and EIN3 TFs that putatively regulate *TET8* (Fig. 6) are involved in the defense response: SR1 suppresses the defense response (Nie et al., 2012), MYB4 is a transcriptional repressor that is induced by the elicitor Flagellin22 (FLG22; Schenke et al., 2011), and EIN3 activates downstream immune-responsive genes in an ethylene-dependent way, such as *FLS2*, which has EIN3-binding sites at the promoter region (Boutrot et al., 2010). *TET8* is up-regulated in the loss-of-function *sr1* allele and down-regulated in the *ein3-1eil1-1* double mutant, indicating that *TET8* expression is antagonistically regulated by SR1 and EIN3 in the immune signaling pathway. *TET8* gene expression was significantly induced by the FLG22 and Elongation Factor Tu (EF-Tu) elicitors that mimicked pathogen infection (Supplemental Fig. S4B), which confirmed the perturbation heat map, the cis-regulatory elements in the promoter region, and the TF-*TET8* gene regulatory network.

In conclusion, combining in planta expression and mutational analyses with meta-analyses on perturbation responses, cis-regulatory element identification, and the construction of a TF-*TET* regulatory network provided an exciting novel and integrated approach, revealing already the function of a few plant tetraspanins and enabling the functional prediction of many more *TET* genes in future work.

MATERIALS AND METHODS

Plant Materials and Growth Conditions

The mutant lines *tet5-1* (GABI-Kat 290A02), *tet5-2* (SALK_148216), *tet5-3* (SALK_020009C), *tet6-1* (SALK_005482C), *tet6-2* (SALK_139305), and *tet13-1* (SALK_011012C) were obtained from Arabidopsis (*Arabidopsis thaliana*) GABI-Kat (http://www.gabi-kat.de/) and the European Arabidopsis Stock Centre (http://www.arabidopsis.org/). The presence of the T-DNA was confirmed by PCR with T-DNA-specific and gene-specific primers (Supplemental Table S3).

Seeds were germinated on Murashige and Skoog medium supplemented with 1% (w/v) Suc and 0.8% (w/v) agarose, pH 5.7. Seeds were surface sterilized

and stratified at 4°C for two nights and moved to the growth chamber. For *pAtTET*::*NLS-GFP/GUS* lines, 6-d-old seedlings grown vertically at 21°C under 24-h light conditions (75–100 μmol m^{-2} s^{-1}) were used for SAM and root analysis; 14-d-old seedlings corresponding to growth stage 1.04 (Boyes et al., 2001) and grown horizontally at 21°C under 16-h-light/8-h-dark conditions were used for cotyledon and emerging leaf 1, 2, 3, and 4 primordia analysis; 6-week-old plants grown in the soil at 21°C under 16-h-light/8-h-dark conditions were used for the analysis of inflorescences, different stages of flowers, siliques, and embryos.

Promoter and Open Reading Frame Cloning, Construction of Expression Vectors, and Plant Transformation

Promoter sequences, defined as intergenic regions with sizes ranging between 396 and 3,400 bp, and open reading frame sequences were amplified from the Arabidopsis genome with the primers listed in Supplemental Table S3 and cloned into the entry vectors using BP Clonase (Invitrogen) to generate the entry clone.

For complementation of *tet13-1*, full-length genomic DNA of *AtTET13* was amplified with the primers listed in Supplemental Table S3 and cloned into the entry vectors using BP Clonase (Invitrogen) to generate the entry clone. The expression clones were constructed by LR Clonase (Invitrogen) with the entry clone and the destination vectors pMK7S*NFm14GW (*pAtTET1-17*::*NLS-GFP/GUS*), pK7FWG2 (*p35S*::*TET3*:*GFP*), and pB2GW7 (*p35S*::*TET13*; Karimi et al., 2007). The plasmids were transferred into *Agrobacterium tumefaciens* pMP90 cells. All constructs were transferred into Arabidopsis ecotype Col-0 or *tet13-1* by floral dip transformation. A total of 25 mg of transgenic seeds of the T1 generation was used for high-density plating on 50 mg L^{-1} kanamycin (*pAtTET1-17*::*NLS-GFP/GUS* and *p35S*::*TET3*:*GFP*) or 7.5 mg L^{-1} DL-phosphinothricin (Duchefa; complementation of *tet13-1* with p*35S*::*TET13*). The resistant seedlings were transferred into soil for T2 generation seed harvest.

For *pAtTET1-17*::*NLS-GFP/GUS* reporter lines, the number of T-DNA loci was analyzed in seven to 35 T2 populations per construct after germination on kanamycin; three lines per construct with a single-locus insertion were analyzed by X-Gluc histochemical staining to score the promoter activity during development. For the complementation analysis of *tet13-1*, T2 seedlings of lines C1 and C5 containing one and two T-DNA loci with p*35S*::*TET13*, respectively, were genotyped for the presence of the *p35S*::*TET13* T-DNA using *bar* primers (Supplemental Table S3) and used for primary root growth and emerged lateral root density measurements.

Histochemical, Histological, and Phenotypic Analyses and Statistical Tests

The X-Gluc assay was performed as described previously (Coussens et al., 2012). Ovules were cleared overnight in an 8:2:1 (g:mL:mL) mixture of chloral hydrate:distilled water:glycerol and mounted on the microscope slides with the same solution (Grini et al., 2002). For the LRP staging and a better visualization of the *TET13* expression pattern in the LRP, the samples were treated as described previously with some modifications (Malamy and Benfey, 1997). Both fresh and stained samples were fixed in 70% (v/v) ethanol overnight and transferred into 4% (v/v) HCl and 20% (v/v) methanol and incubated at 62°C for 40 min in 7% (w/v) NaOH and 60% (v/v) ethanol at room temperature for 15 min. The samples were then rehydrated for 10 min in 60%, 40%, 20%, or 10% (v/v) ethanol at room temperature. Finally, the samples were infiltrated in 25% (v/v) glycerol and 5% (v/v) ethanol for 10 min and mounted with 50% (v/v) glycerol. The root meristem size was determined as the number of cells in the cortex cell file from the QC to the first elongated cell (Casamitjana-Martínez et al., 2003). The samples were mounted with 50% (v/v) lactic acid and observed immediately. For the hydroxyurea, NAA, and NPA treatments, 5-d-old seedlings were transferred onto Murashige and Skoog (MS) medium supplemented for 24 h with 1 mM hydroxyurea, 1 μM NAA, or 1 μM NPA, respectively. Seedlings treated with hydroxyurea were counterstained with propidium iodide and observed with a confocal microscope. Seedlings treated with NAA or NPA were also treated for 1 min with Lugol solution to stain the starch granules, mounted with chloral hydrate, and checked immediately with the microscope.

For epidermal cell imaging, leaves were fixed in 100% ethanol overnight and mounted with 90% (v/v) lactic acid. The leaf area was measured with the ImageJ software (http://rsbweb.nih.gov/ij/). The epidermal cells on the abaxial side were drawn with a Leica DMLB microscope equipped with a drawing tube and differential interference contrast objectives. The total number of cells per leaf was determined as described previously (De Veylder et al., 2001).

All samples were imaged with a binocular Leica microscope or an Olympus DIC-BX51 microscope. The confocal images were taken with an Olympus Fluo View FV1000 microscope or a Zeiss LSM5 Exiter confocal microscope. The fluorescence was detected after a 488-nm (GFP) or 543-nm (propidium iodide) excitation and an emission of 495 to 520 nm for GFP or 590 to 620 nm for propidium iodide. Transverse sectioning was done according to De Smet et al. (2004).

Means between samples were compared by a two-tailed Student's *t* test; an *f* test was assessed for the equality between population variances.

Elicitor Treatment

EF-Tu and FLG22 were synthesized and purchased from GenScript (http://www.genscript.com). Col-0 plant samples were grown on MS medium for 16 d and transferred into liquid MS medium supplemented with EF-Tu or FLG22 at the final concentration of 1 μM for 2 h on an orbital shaker.

Quantitative Real-Time PCR Analysis

Total RNA was prepared with the RNeasy kit (Qiagen). One microgram of RNA was used as a template to synthesize complementary DNA with the iScript cDNA Synthesis Kit (Bio-Rad). The expression level was analyzed on a LightCycler 480 apparatus (Roche) with SYBR Green, and all reactions were performed in three technical replicates. Expression levels were normalized to reference genes *PROTEIN PHOSPHATASE 2A SUBUNIT A3* and *UBIQUITIN-CONJUGATING ENZYME21* (Czechowski et al., 2005).

cis-Regulatory Element Analysis

Known TF-binding sites and DNA motifs were mapped on the 2-kb upstream sequence for all genes and for all included species using DNA-pattern allowing no mismatches (Thomas-Chollier et al., 2008). A total of 692 cis-regulatory elements were obtained from AGRIS (Davuluri et al., 2003), PLACE (Higo et al., 1999), and Athamap (Steffens et al., 2004). In addition, 44 positional count matrices were obtained from Athamap, and for 15 TFs, positional count matrices were obtained from ChIP sequencing data (Heyndrickx et al., 2014). Positional count matrices were mapped genome wide using MatrixScan using a cutoff value of $P < 1e\text{-}05$ (Thomas-Chollier et al., 2008). In order to reduce the high false positive rates associated with interfering regulatory interactions based on simple motif mapping, two types of filtering were used. A first approach to enrich for functional interactions consisted of filtering motif matches using cross-species sequence conservation or open chromatin regions. Therefore, motif matches were filtered using conserved noncoding sequences (Van de Velde et al., 2014) and DH sites. The DH sites were downloaded from the National Center for Biotechnology Information Sequence Read Archive database (accession no. SRP009678; Zhang et al., 2012). A second approach started from tightly coregulated genes to identify coregulatory motifs or TF-binding sites. For each *TET* gene, motif-mapping information was combined with a set of coregulated genes from Genevestigator. In the perturbations tool, the perturbations under which *TET* genes were two times up-regulated ($P < 0.05$) were selected to create new sample sets. Then, in the coexpression tool, the top 200 positively correlated genes under the categories anatomy and perturbations were selected. The overlapping genes were defined as coregulated genes. Only motifs present in the upstream or downstream *TET* sequence and showing significant enrichment in the coregulation cluster were retained. Motif enrichment was determined using the hypergeometric distribution using false discovery rate correction. Only significantly ($P < 0.05$) enriched motifs were retained.

Gene Regulatory Network Inference

The gene regulatory networks based on conserved noncoding sequences from Van de Velde et al. (2014) and on TF ChIP data from Heyndrickx et al. (2014) were filtered for TET target genes. For TFs with ChIP data, differentially expressed genes after TF perturbation were also included for AT5G13790 (AGL15; Zheng et al., 2009), AT1G19350 (BES1; Yu et al., 2011), AT5G61850 (LFY; Schmid et al., 2003), and AT3G26790 (FUS3; Yamamoto et al., 2010; Lumba et al., 2012). For other TFs, differentially expressed genes after TF perturbation were obtained through Genevestigator.

Gene Ontology Enrichment

Gene Ontology enrichment was performed using the hypergeometric distribution with Bonferroni correction.

Supplemental Data

The following supplemental materials are available.

Supplemental Figure S1. *TET* expression in seedlings and seeds and TET3 protein localization.

Supplemental Figure S2. *TET* expression in flower organs.

Supplemental Figure S3. *tet13-1* primary root morphology.

Supplemental Figure S4. *tet5* and *tet6* single and double mutant phenotypes in other alleles.

Supplemental Figure S5. Heat map of *TET* responses to different perturbations and *TET8* expression levels after elicitor treatment.

Supplemental Table S1. *tet* mutants collected in this study.

Supplemental Table S2. *TET* cis-regulatory element information.

Supplemental Table S3. Primers used in the study.

Supplemental Movie S1. TET3-GFP movement on the plasma membrane.

ACKNOWLEDGMENTS

We thank Annick Bleys for help in preparing the article, Matyas Fendrych for help in confocal imaging, and Carina Braeckman for plant transformation.

Received August 19, 2015; accepted September 26, 2015; published September 28, 2015.

LITERATURE CITED

Adamczyk BJ, Lehti-Shiu MD, Fernandez DE (2007) The MADS domain factors AGL15 and AGL18 act redundantly as repressors of the floral transition in Arabidopsis. Plant J **50:** 1007–1019

Aerts S (2012) Computational strategies for the genome-wide identification of *cis*-regulatory elements and transcriptional targets. Curr Top Dev Biol **98:** 121–145

Benková E, Michniewicz M, Sauer M, Teichmann T, Seifertová D, Jürgens G, Friml J (2003) Local, efflux-dependent auxin gradients as a common module for plant organ formation. Cell **115:** 591–602

Boavida LC, Qin P, Broz M, Becker JD, McCormick S (2013) Arabidopsis tetraspanins are confined to discrete expression domains and cell types in reproductive tissues and form homo- and heterodimers when expressed in yeast. Plant Physiol **163:** 696–712

Boutrot F, Segonzac C, Chang KN, Qiao H, Ecker JR, Zipfel C, Rathjen JP (2010) Direct transcriptional control of the *Arabidopsis* immune receptor FLS2 by the ethylene-dependent transcription factors EIN3 and EIL1. Proc Natl Acad Sci USA **107:** 14502–14507

Boyes DC, Zayed AM, Ascenzi R, McCaskill AJ, Hoffman NE, Davis KR, Görlach J (2001) Growth stage-based phenotypic analysis of *Arabidopsis*: a model for high throughput functional genomics in plants. Plant Cell **13:** 1499–1510

Casamitjana-Martínez E, Hofhuis HF, Xu J, Liu CM, Heidstra R, Scheres B (2003) Root-specific *CLE19* overexpression and the *sol1/2* suppressors implicate a CLV-like pathway in the control of *Arabidopsis* root meristem maintenance. Curr Biol **13:** 1435–1441

Chandrasekharan MB, Bishop KJ, Hall TC (2003) Module-specific regulation of the β-phaseolin promoter during embryogenesis. Plant J **33:** 853–866

Chiu WH, Chandler J, Cnops G, Van Lijsebettens M, Werr W (2007) Mutations in the *TORNADO2* gene affect cellular decisions in the peripheral zone of the shoot apical meristem of *Arabidopsis thaliana*. Plant Mol Biol **63:** 731–744

Cnops G, Neyt P, Raes J, Petrarulo M, Nelissen H, Malenica N, Luschnig C, Tietz O, Ditengou F, Palme K, et al (2006) The *TORNADO1* and *TORNADO2* genes function in several patterning processes during early leaf development in *Arabidopsis thaliana*. Plant Cell **18:** 852–866

Cnops G, Wang X, Linstead P, Van Montagu M, Van Lijsebettens M, Dolan L (2000) *Tornado1* and *tornado2* are required for the specification of radial and circumferential pattern in the *Arabidopsis* root. Development **127:** 3385–3394

Coussens G, Aesaert S, Verelst W, Demeulenaere M, De Buck S, Njuguna E, Inzé D, Van Lijsebettens M (2012) *Brachypodium distachyon* promoters as efficient building blocks for transgenic research in maize. J Exp Bot **63:** 4263–4273

Czechowski T, Stitt M, Altmann T, Udvardi MK, Scheible WR (2005) Genome-wide identification and testing of superior reference genes for transcript normalization in Arabidopsis. Plant Physiol **139:** 5–17

Davuluri RV, Sun H, Palaniswamy SK, Matthews N, Molina C, Kurtz M, Grotewold E (2003) AGRIS: Arabidopsis Gene Regulatory Information Server, an information resource of Arabidopsis *cis*-regulatory elements and transcription factors. BMC Bioinformatics **4:** 25

De Rybel B, Möller B, Yoshida S, Grabowicz I, Barbier de Reuille P, Boeren S, Smith RS, Borst JW, Weijers D (2013) A bHLH complex controls embryonic vascular tissue establishment and indeterminate growth in Arabidopsis. Dev Cell **24:** 426–437

De Smet I, Chaerle P, Vanneste S, De Rycke R, Inzé D, Beeckman T (2004) An easy and versatile embedding method for transverse sections. J Microsc **213:** 76–80

De Smet I, Tetsumura T, De Rybel B, Frei dit Frey N, Laplaze L, Casimiro I, Swarup R, Naudts M, Vanneste S, Audenaert D, et al (2007) Auxin-dependent regulation of lateral root positioning in the basal meristem of *Arabidopsis*. Development **134:** 681–690

De Veylder L, Beeckman T, Beemster GT, Krols L, Terras F, Landrieu I, van der Schueren E, Maes S, Naudts M, Inzé D (2001) Functional analysis of cyclin-dependent kinase inhibitors of *Arabidopsis*. Plant Cell **13:** 1653–1668

Ding Z, Friml J (2010) Auxin regulates distal stem cell differentiation in *Arabidopsis* roots. Proc Natl Acad Sci USA **107:** 12046–12051

Ezcurra I, Wycliffe P, Nehlin L, Ellerström M, Rask L (2000) Transactivation of the *Brassica napus* napin promoter by ABI3 requires interaction of the conserved B2 and B3 domains of ABI3 with different *cis*-elements: B2 mediates activation through an ABRE, whereas B3 interacts with an RY/G-box. Plant J **24:** 57–66

Fernandez-Calvino L, Faulkner C, Walshaw J, Saalbach G, Bayer E, Benitez-Alfonso Y, Maule A (2011) Arabidopsis plasmodesmal proteome. PLoS One **6:** e18880

Fradkin LG, Kamphorst JT, DiAntonio A, Goodman CS, Noordermeer JN (2002) Genomewide analysis of the *Drosophila* tetraspanins reveals a subset with similar function in the formation of the embryonic synapse. Proc Natl Acad Sci USA **99:** 13663–13668

Goldberg AFX (2006) Role of peripherin/rds in vertebrate photoreceptor architecture and inherited retinal degenerations. Int Rev Cytol **253:** 131–175

Grini PE, Jürgens G, Hülskamp M (2002) Embryo and endosperm development is disrupted in the female gametophytic *capulet* mutants of Arabidopsis. Genetics **162:** 1911–1925

Heyndrickx KS, Van de Velde J, Wang C, Weigel D, Vandepoele K (2014) A functional and evolutionary perspective on transcription factor binding in *Arabidopsis thaliana*. Plant Cell **26:** 3894–3910

Higo K, Ugawa Y, Iwamoto M, Korenaga T (1999) Plant cis-acting regulatory DNA elements (PLACE) database: 1999. Nucleic Acids Res **27:** 297–300

Himanen K, Boucheron E, Vanneste S, de Almeida Engler J, Inzé D, Beeckman T (2002) Auxin-mediated cell cycle activation during early lateral root initiation. Plant Cell **14:** 2339–2351

Huang S, Yuan S, Dong M, Su J, Yu C, Shen Y, Xie X, Yu Y, Yu X, Chen S, et al (2005) The phylogenetic analysis of tetraspanins projects the evolution of cell-cell interactions from unicellular to multicellular organisms. Genomics **86:** 674–684

Kaji K, Oda S, Miyazaki S, Kudo A (2002) Infertility of CD9-deficient mouse eggs is reversed by mouse CD9, human CD9, or mouse CD81: polyadenylated mRNA injection developed for molecular analysis of sperm-egg fusion. Dev Biol **247:** 327–334

Karimi M, Bleys A, Vanderhaeghen R, Hilson P (2007) Building blocks for plant gene assembly. Plant Physiol **145:** 1183–1191

Kasahara RD, Portereiko MF, Sandaklie-Nikolova L, Rabiger DS, Drews GN (2005) *MYB98* is required for pollen tube guidance and synergid cell differentiation in *Arabidopsis*. Plant Cell **17:** 2981–2992

Krogh A, Larsson B, von Heijne G, Sonnhammer ELL (2001) Predicting transmembrane protein topology with a hidden Markov model: application to complete genomes. J Mol Biol **305:** 567–580

Kumar SV, Lucyshyn D, Jaeger KE, Alós E, Alvey E, Harberd NP, Wigge PA (2012) Transcription factor PIF4 controls the thermosensory activation of flowering. Nature **484:** 242–245

Lieber D, Lora J, Schrempp S, Lenhard M, Laux T (2011) *Arabidopsis WIH1* and *WIH2* genes act in the transition from somatic to reproductive cell fate. Curr Biol **21:** 1009–1017

Lumba S, Tsuchiya Y, Delmas F, Hezky J, Provart NJ, Shi Lu Q, McCourt P, Gazzarrini S (2012) The embryonic leaf identity gene *FUSCA3* regulates vegetative phase transitions by negatively modulating ethylene-regulated gene expression in Arabidopsis. BMC Biol **10:** 8

Luo XM, Lin WH, Zhu S, Zhu JY, Sun Y, Fan XY, Cheng M, Hao Y, Oh E, Tian M, et al (2010) Integration of light- and brassinosteroid-signaling pathways by a GATA transcription factor in *Arabidopsis*. Dev Cell **19:** 872–883

Malamy JE, Benfey PN (1997) Organization and cell differentiation in lateral roots of *Arabidopsis thaliana*. Development **124:** 33–44

Mejia-Guerra MK, Pomeranz M, Morohashi K, Grotewold E (2012) From plant gene regulatory grids to network dynamics. Biochim Biophys Acta **1819:** 454–465

Moore RC, Purugganan MD (2005) The evolutionary dynamics of plant duplicate genes. Curr Opin Plant Biol **8:** 122–128

Murray JAH, Jones A, Godin C, Traas J (2012) Systems analysis of shoot apical meristem growth and development: integrating hormonal and mechanical signaling. Plant Cell **24:** 3907–3919

Nakamichi N, Kita M, Niinuma K, Ito S, Yamashino T, Mizoguchi T, Mizuno T (2007) *Arabidopsis* clock-associated pseudo-response regulators PRR9, PRR7 and PRR5 coordinately and positively regulate flowering time through the canonical CONSTANS-dependent photoperiodic pathway. Plant Cell Physiol **48:** 822–832

Nie H, Zhao C, Wu G, Wu Y, Chen Y, Tang D (2012) SR1, a calmodulin-binding transcription factor, modulates plant defense and ethylene-induced senescence by directly regulating *NDR1* and *EIN3*. Plant Physiol **158:** 1847–1859

Perilli S, Di Mambro R, Sabatini S (2012) Growth and development of the root apical meristem. Curr Opin Plant Biol **15:** 17–23

Pillitteri LJ, Torii KU (2012) Mechanisms of stomatal development. Annu Rev Plant Biol **63:** 591–614

Riou-Khamlichi C, Menges M, Healy JMS, Murray JAH (2000) Sugar control of the plant cell cycle: differential regulation of *Arabidopsis* D-type cyclin gene expression. Mol Cell Biol **20:** 4513–4521

Rubinstein E, Ziyyat A, Prenant M, Wrobel E, Wolf JP, Levy S, Le Naour F, Boucheix C (2006) Reduced fertility of female mice lacking CD81. Dev Biol **290:** 351–358

Sarkar AK, Luijten M, Miyashima S, Lenhard M, Hashimoto T, Nakajima K, Scheres B, Heidstra R, Laux T (2007) Conserved factors regulate signalling in *Arabidopsis thaliana* shoot and root stem cell organizers. Nature **446:** 811–814

Schenke D, Böttcher C, Scheel D (2011) Crosstalk between abiotic ultraviolet-B stress and biotic (flg22) stress signalling in *Arabidopsis* prevents flavonol accumulation in favor of pathogen defence compound production. Plant Cell Environ **34:** 1849–1864

Schmid M, Uhlenhaut NH, Godard F, Demar M, Bressan R, Weigel D, Lohmann JU (2003) Dissection of floral induction pathways using global expression analysis. Development **130:** 6001–6012

Sparks E, Wachsman G, Benfey PN (2013) Spatiotemporal signalling in plant development. Nat Rev Genet **14:** 631–644

Steffens NO, Galuschka C, Schindler M, Bülow L, Hehl R (2004) AthaMap: an online resource for in silico transcription factor binding sites in the *Arabidopsis thaliana* genome. Nucleic Acids Res **32:** D368–D372

Swarup K, Benková E, Swarup R, Casimiro I, Péret B, Yang Y, Parry G, Nielsen E, De Smet I, Vanneste S, et al (2008) The auxin influx carrier LAX3 promotes lateral root emergence. Nat Cell Biol **10:** 946–954

Thomas-Chollier M, Sand O, Turatsinze JV, Janky R, Defrance M, Vervisch E, Brohée S, van Helden J (2008) RSAT: regulatory sequence analysis tools. Nucleic Acids Res **36:** W119–W127

van den Berg C, Willemsen V, Hendriks G, Weisbeek P, Scheres B (1997) Short-range control of cell differentiation in the *Arabidopsis* root meristem. Nature **390:** 287–289

Vandepoele K, Quimbaya M, Casneuf T, De Veylder L, Van de Peer Y (2009) Unraveling transcriptional control in Arabidopsis using cis-regulatory elements and coexpression networks. Plant Physiol **150:** 535–546

Van de Velde J, Heyndrickx KS, Vandepoele K (2014) Inference of transcriptional networks in *Arabidopsis* through conserved noncoding sequence analysis. Plant Cell **26:** 2729–2745

Wang F, Vandepoele K, Van Lijsebettens M (2012) Tetraspanin genes in plants. Plant Sci **190:** 9–15

Yamamoto A, Kagaya Y, Usui H, Hobo T, Takeda S, Hattori T (2010) Diverse roles and mechanisms of gene regulation by the Arabidopsis seed maturation master regulator FUS3 revealed by microarray analysis. Plant Cell Physiol **51:** 2031–2046

Yáñez-Mó M, Barreiro O, Gordon-Alonso M, Sala-Valdés M, Sánchez-Madrid F (2009) Tetraspanin-enriched microdomains: a functional unit in cell plasma membranes. Trends Cell Biol **19:** 434–446

Yu X, Li L, Zola J, Aluru M, Ye H, Foudree A, Guo H, Anderson S, Aluru S, Liu P, et al (2011) A brassinosteroid transcriptional network revealed by genome-wide identification of BESI target genes in *Arabidopsis thaliana*. Plant J **65:** 634–646

Zhang W, Zhang T, Wu Y, Jiang J (2012) Genome-wide identification of regulatory DNA elements and protein-binding footprints using signatures of open chromatin in *Arabidopsis*. Plant Cell **24:** 2719–2731

Zheng Y, Ren N, Wang H, Stromberg AJ, Perry SE (2009) Global identification of targets of the *Arabidopsis* MADS domain protein AGAMOUS-Like15. Plant Cell **21:** 2563–2577